Inorganic Chemistry
Cite This: Inorg. Chem. XXXX, XXX, XXX−XXX
Communication
pubs.acs.org/IC

Fe_5Mo Cluster with Iron-Carbide and Molybdenum-Carbide Bonding Motifs: Structure and Selective Alkyne Reductions

Chris Joseph, Subramaniam Kuppuswamy, Vincent M. Lynch, and Michael J. Rose*

Department of Chemistry, The University of Texas at Austin, Austin, Texas 78712, United States

Supporting Information

ABSTRACT: Herein we report the synthesis, X-ray structure, and characterization of the title pentairon (molybdo)carbido cluster. The reaction of the pentairon (μ_5-carbido) dianion $[Fe_5(\mu_6\text{-}C)(\mu_2\text{-}CO)_2(CO)_{12}]^{2-}$ (**1**) with $[Mo(CO)_3(chpt)]$ (chpt = cycloheptatriene) forms the heterohexanuclear cluster $[K(benzo\text{-}18\text{-}crown\text{-}6)]_2[Fe_5Mo(\mu_6\text{-}C)(\mu_2\text{-}CO)_3(CO)_{14}]$ (**2**). The dianion exhibits a $Fe_5Mo(\mu_6\text{-}C)$ core structure supported by three bridging (ν_{CO} = 1788 cm^{-1}) and terminal (ν_{CO} = 1943 cm^{-1}) CO ligands. Cluster **2** provides the selective reduction of diphenylacetylene to *cis*-diphenylethylene via a spectroscopically observed cluster-hydride intermediate (^{1}H NMR: δ −26).

Since the discovery of small-molecule metal clusters with interstitial light atoms in 1962, the encapsulation of light atoms inside metal clusters has remained a fascinating curiosity in inorganic chemistry.[1] The seminal work by Churchill and others involving caged carbides, nitrides, and oxides brought forth new structural possibilities and new routes of studying heterogeneous metallic reaction pathways in small-molecule format.[2−6] Additionally, the recent discovery and confirmation of the interstitial carbide present in the FeMoco active site of molybdenum-containing nitrogenase have brought renewed attention to this structural motif.[7,8] For example, recent structural and spectroscopic investigations by DeBeer et al. have led to insight into the electronic structure and spectroscopic signature of an interstitial carbide.[9] Additionally, recent work by Berben et al. using $[Fe_4]$ and $[Fe_5]$ nitrides and carbides has shown their utility in selective CO_2 reduction.[10]

In our research into the synthesis of such metal carbido clusters and nitrogenase, we have investigated the incorporation of "heterometals" into otherwise all-iron carbido clusters. In this work, we report the synthesis, characterization, and X-ray structure of a stable pentairon (molybdo)carbidocarbonyl cluster. While the $[NEt_4]_2$ salt of the title pentairon molybdocarbidocarbonyl cluster has been reported before,[11] the full structure of the cluster is not available in the CCDC. Our attempts to characterize this compound produced a structure in the cubic space group $Fm\bar{3}m$, wherein the high-symmetry gives rise to ambiguous metal atom identities. We do note, however, that the structure of the $[Fe_5Mo]$ cluster can be inferred from its gold-coordinated derivatives.[6] In this work, we show that, by inducing an interaction between the cluster and its counterion, a crystal structure with unambiguous metal ion identities is obtained. Finally, the cluster is demonstrated to perform selective reductions with the model substrate diphenylacetylene (DPA).

It was necessary to modify the preparation of several reported clusters to facilitate crystallization and structure solution along the synthetic pathway to the final molybdenum-containing cluster. The neutral species $[Fe_5(\mu_5\text{-}C)(CO)_{15}]$ (prepared according to refs 11 and 12) was reduced with 2.1 equiv of KC_8 in tetrahydrofuran (THF; Scheme 1), followed by filtration of the reaction solution and the addition of 2.1 equiv of benzo-18-crown-6. Subsequent crystallization in FPh/Et_2O afforded black plates of $[K(benzo\text{-}18\text{-}crown\text{-}6)]_2[Fe_5(\mu_5\text{-}C)(CO)_{14}]$ (**1**; Figure S9), which exhibits a *nido*-$[Fe_5(\mu_5\text{-}C)]$ core motif with an open site at the basal position of the carbide similar to the $[NEt_4]_2$ salt.[10,12] According to previous precedents,[6,13] we reasoned that the open carbide dative site could be capped with a heterometal to afford the corresponding Fe_5M carbide structure. We thus attempted metalation of the carbide with chromium, molybdenum, and tungsten carbonyls. Reactions of $[M(CO)_3(L)]$ [where L = chpt (cycloheptatriene) or $(THF)_3$] with M = Cr and Mo in THF afforded adducts postulated as $[Fe_5M(\mu_6\text{-}C)(CO)_{17}]^{2-}$, as judged by their IR spectra (blue-shifted features ≈ 1940 and 1785 cm^{-1}). However, whereas the Mo adduct proved stable under crystallization conditions, the $\{Cr(CO)_3\}$ unit spontaneously dissociated over time, even at low temperatures (−30 °C) during crystallization. Treatment of **1** with $[W(CO)_3(THF)_3]$ did not install the $\{W(CO)_3\}$ unit to the carbide site under any tested condition, possibly because of the poor orbital overlap between the diffuse W 5d set and the contracted C 2p set.

Scheme 1. Reaction of 1 with $[M(CO)_3(L)]$ [L = chpt or $(THF)_3$], Which in the Case of M = Mo and L = chpt Affords the Title Cluster 2

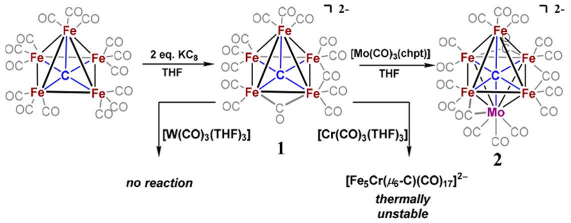

On the basis of the stability of the $[Fe_5Mo]^{2-}$ cluster, structural characterization was forthcoming (FPh/Et_2O vapor diffusion), affording black plates of $[K(benzo\text{-}18\text{-}crown\text{-}6)]_2[Fe_5Mo(\mu_6\text{-}$

Received: October 12, 2017

DOI: 10.1021/acs.inorgchem.7b02615
Inorg. Chem. XXXX, XXX, XXX−XXX

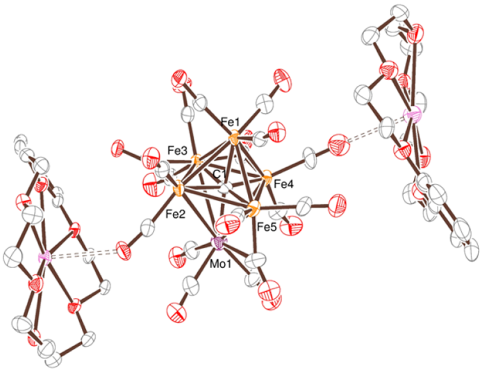

Figure 1. ORTEP diagram (50% thermal ellipsoids) for **2**. Bond distances (Å): Mo1−C1 = 2.113(6), $Fe1_{ax}$−C1 = 1.937(6), Fe2−C1 = 1.896(5), Fe3−C1 = 1.902(4), Fe4−C1 = 1.887(5), Fe5−C1 = 1.881(4), Mo1−Fe2 = 2.9666(9), Mo1−Fe3 = 3.054(1), Mo1−Fe4 = 2.861(1), Mo1−Fe5 = 2.769(1), Mo1−$C16_{term}$ = 1.972(7), Mo1−$C17_{term}$ = 1.961(7), Mo1−$C18_{term}$ = 1.961(8), Mo1−$C15_{bridg}$ = 2.344(6), K1⋯O5 = 2.831(5), K2⋯O11 = 2.916(8).

C)(μ_2-CO)$_3$(CO)$_{14}$] (**2**; Figure 1). The structure exhibits a "capped" μ_6-carbide motif, incorporating the {Mo(CO)$_3$} unit at a distance of 2.113(6) Å from the carbide. Regarding the *trans* effect of the capping {Mo(CO)$_3$} unit, the apical Fe ion is substantially compressed toward the carbide at Fe−carbide = 1.937(6) Å versus the five-iron cluster [1.99(1) Å];[12] the equatorial Fe−carbide distances remain largely unchanged. The Mo site exhibits three terminal CO ligands [Mo−C(O) = 1.972(7), 1.961(7), and 1.961(8) Å] and one bridging CO ligand [Mo−C(O) = 2.344(6) Å] with Fe5.

Overall, the Mo center participates in nine bonding interactions (including one bridging CO), whereas the highest-coordination-number Fe site (Fe3; also coordination number = 9) exhibits two bridging CO ligands. Thus, while polyhedral skeletal electron pair theory (PSEPT) accurately predicts the total number of CO ligands, simple inspection of the metal oxidation states [Mo^0 versus Fe^I] indicates the location of the "extra" CO on the Mo site. Incubation of **2** under a CO atmosphere results in no change in the IR spectrum or enhanced features in the ^{13}C NMR, indicating no further CO binding and the validity of the PSEPT rules in this case. The bond metrics of the terminal and bridging CO ligands on the Fe sites remain largely unchanged [avg Fe−C(O)$_{term}$ = 1.778 ± 0.017; Fe−C(O)$_{bridg}$ = 1.968 ± 0.141 Å]. Lastly, the crowned K ions exhibit close contacts with two terminal CO ligands [K⋯O = 2.831(5) and 2.916(8) Å], similar to the K⋯O contacts found in **1**.

To probe the redox activity of **1** and **2**, we performed cyclic voltammetry (CV) to determine the accessibility of the reduced congeners of **1** and **2**. A cathodic sweep of **1** in THF (Figure S4) did not exhibit any reduction events. The return anodic sweep, however, did reveal two oxidation events assigned to the conversion of the dianionic cluster to the known neutral species. Alternately, the CV for the Mo-containing cluster **2** (Figure S8) revealed a set of reversible features with a reduction event at −2.00 versus Fc. The accessibility of these redox events to common chemical reductants, such as KC_8 and sodium perylenide (Na_2Per), led us to explore reactions of the reduced cluster with model substrates that provide insight into selective reductions of triply bonded functional groups.

On the basis of these findings and literature precedent demonstrating the activation of alkynes by iron carbonyls,[14] we pursued reactions of the model substrate DPA with each cluster under reducing conditions in the presence of varying proton sources. Selected results are delineated in Table 1 (additional results in Table S3). Previous studies explored the reduction of DPA using palladium-catalyzed or electrochemical means to obtain *cis*-alkene.[15] In contrast, there is just a single report of a single-molecule catalyst (an [Fe_4S_4](SR)$_4$]$^{2-}$ cluster) for DPA reduction.[16] A general, unbalanced formula for the reaction performed here is given as:

$$[\text{cluster}] + 30\,e^- + 30\,H^+ + 15\,C{\equiv}C \rightarrow$$

$$\textit{cis-}C{=}C + \textit{trans-}C{=}C + C{-}C$$

First, control reactions with no cluster (KC_8, LutH·OTf) revealed a poorly selective 0.25 ratio of the intermediately reduced product (diphenylethylene) to the fully reduced alkane product (diphenylethane) with 21.8% DPA conversion. None of the desired *cis*-alkene was observed in the control reaction. In contrast, the presence of catalytic **2** (KC_8, LutH·OTf) provided better selectivity for alkene/alkane conversion (1.58 ratio), indicating over a 6-fold improvement in the selectivity, despite a diminished 14.1% overall conversion. Within the possible alkene products (*trans* and *cis*), cluster **2** did provide some, albeit minimal, *cis* product (*cis*/*trans* = 0.22). A secondary control reaction replaced cluster **2** as a catalyst with its individual metal center components. When 5 equiv of Fe(CO)$_5$ was used in conjugation with 1 equiv of Mo(CO)$_6$, moderate selectivity was maintained. However, substrate conversion decreased dramatically (3.6%). A screening of different proton sources revealed poor activity with phenols (Table S3) and more consistently beneficial results using nitrogen-based acids. Additionally, it was found that bulkier, lower pK_a proton sources yielded higher

Table 1. Selected Results from Reductions of DPA to *cis*/*trans*-Diphenylethylene and Diphenylethane[a]

catalyst	reductant	proton source	pK_a	temp (°C)	convn (%)	C=C/C—C ratio	*cis*/*trans* ratio
none	KC_8	[LutH]OTf	6.60	rt	21.8	0.25	0.00
Fe_5 (1)	KC_8	[LutH]OTf	6.60	rt	9.7	0.60	0.34
Fe_5Mo (2)	KC_8	[LutH]OTf	6.60	rt	14.1	1.58	0.22
5Fe + Mo	KC_8	[LutH]OTf	6.60	rt	3.6	0.62	0.82
Fe_5Mo (2)	KC_8	[MesNH$_3$]OTf	4.37	rt	25.4	0.36	0.30
Fe_5Mo (2)	Na_2(Per)	[MesNH$_3$]OTf	4.37	rt	17.9	3.01	0.56
Fe_5Mo (2)	Na_2(Per)	[MesNH$_3$]OTf	4.37	−20	**28.8**	1.66	0.03
Fe_5Mo (2)	Na_2(Per)	[MesNH$_3$]OTf	4.37	60	3.7	6.55	**1.15**
Fe_5Mo (2)	Na_2(Per)	[2,4,6-^{t}Bu$_3$PhNH$_3$]OTf	3.30	rt	15.9	**16.0**	0.65
none	Na_2(Per)	[2,4,6-^{t}Bu$_3$PhNH$_3$]OTf	3.30	rt	0.8	C=C only	0

[a] LutH = 2,6-lutidinium; MesNH$_3$ = 2,4,6-trimethylanilinium; Na_2(Per) = sodium perylenide; 5Fe + Mo = 5Fe(CO)$_5$ + Mo(CO)$_6$; **Fe_5** = cluster **1**; **Fe_5Mo** = cluster **2**. The bold values denote the best result in each column. A complete table of results can be found in the Supporting Information.

substrate conversion and *cis* selectivity. In particular, a sterically encumbered anilinium triflate (2,4,6-trimethylanilinium triflate) provided the highest overall conversion (25.4%), moderate alkene/alkane selectivity (0.36), and a higher *cis*/*trans* ratio (0.30) than other conditions. By comparison, the Fe-only cluster **1** provided a low overall conversion (9.7%) and only an intermediate alkene/alkane selectivity (0.60). The less beneficial results from **1** are most likely due to its inaccessible redox activity by KC_8 and the decreased stability of the $[Fe_5]$ core versus the $[Fe_5Mo]$ core under catalytic conditions.

To further optimize the conversion and selectivity of the reaction, a weaker reducing agent (sodium perylenide, generated in situ) was used. While substrate conversion dropped modestly (from 25% to 18%), the selectivity of *cis*-alkene increased significantly (alkene/alkane = 3.01; *cis*/*trans* = 0.56). Interestingly, temperature was found to be inversely correlated with substrate conversion while being directly correlated with selectivity toward *cis*-alkene. Performing the reaction at 60 °C exhibited the highest selectivity (alkene/alkane = 6.55; *cis*/*trans* = 1.15), although it suffered from poor substrate conversion (3.7%). Finally, 2,4,6-tri-*tert*-butylanilinium triflate was used as an even bulkier proton source, which dramatically increased the alkene/alkane selectivity (16.0) while the overall conversion and *cis* selectivity remained moderate. The corresponding control reaction (no catalyst) provided only 0.8% overall conversion, and no *cis* product was detected.

To establish the integrity of the cluster throughout the catalytic process, we determined several spectroscopic properties of the in situ cluster product. After catalysis with **2**, the IR spectrum of the reaction mixture exhibited a distinct ν_{CO} feature at 1963 cm^{-1} (Figure S11); this is distinct from the starting IR of **2**, at 1943 cm^{-1} (Figure S7). To provide context for this observation and to gain insight into the mechanism of substrate reaction, stoichiometric reactions of **2** with reductants and substrates were performed (Figure S12). Treatment of cluster **2** with 1 equiv of $Na_2(Per)$ resulted in a blue shift to 1958 cm^{-1}. Subsequent addition of 1 equiv of DPA resulted in no significant change (ν_{CO} at 1959 cm^{-1}), indicating no direct interaction of reduced **2** with DPA. In contrast, treatment of reduced **2** with 1 equiv of $[MesNH_3]OTf$ resulted in a slightly shifted ν_{CO} at 1962 cm^{-1} (closer to the crude mixture value of 1963 cm^{-1}), indicating direct reaction of reduced **2** with the proton source. Also, while the ^1H NMR spectrum of this anilinium-treated solution did not exhibit a hydride resonance, treatment of the solution with a stronger acid (TfOH) did afford a distinct hydride resonance at −26 ppm (Figure S13), attributed to the formation of a bridging hydride species (IR: ν_{CO} = 1962 cm^{-1}). This feature is analogous to protonation of the corresponding $[Fe_6]^{4-}$ species, which also affords a bridging hydride (−21 ppm).[17] Overall, it can be postulated that the cluster core structure is maintained throughout catalysis and that the primary mechanism of substrate reduction proceeds through a cluster−hydride intermediate that acts upon the DPA substrate.

In summary, we have structurally characterized a K-crown-supported, carbide-based metallocluster (**2**) that exhibits a molybdenum-carbide motif and five iron-carbide bonds. The accessible reduction potential of **2** allows for activation with sodium perylinide and protonation to afford the corresponding cluster−hydride species; this provides enhanced selectivity in the reduction of DPA to the *cis*-alkene product. More broadly, the Mo···Fe distances found in **2** (2.77−3.05 Å) are only slightly longer than those found in the FeMoco cluster (~2.7 Å), thus providing an interesting comparison to the carbide−sulfide-supported FeMoco cluster in nitrogenase. More synthetic work is needed to address the substitution of terminal and bridging CO units to biologically relevant, sulfur-based supports such as sulfides, thiolates, and thioethers. This work is now underway and will be reported in due course.

■ ASSOCIATED CONTENT

Ⓢ Supporting Information

The Supporting Information is available free of charge on the ACS Publications website at DOI: 10.1021/acs.inorgchem.7b02615.

Syntheses, NMR, IR, CV, X-ray experimental and parameters, and tabulated bond distances (PDF)

Accession Codes

CCDC 1541349 contains the supplementary crystallographic data for this paper. These data can be obtained free of charge via www.ccdc.cam.ac.uk/data_request/cif, or by emailing data_request@ccdc.cam.ac.uk, or by contacting The Cambridge Crystallographic Data Centre, 12 Union Road, Cambridge CB2 1EZ, UK; fax: +44 1223 336033.

■ AUTHOR INFORMATION

Corresponding Author

*E-mail: mrose@cm.utexas.edu (M.J.R.).

ORCID

Chris Joseph: 0000-0002-9763-5162
Michael J. Rose: 0000-0002-6960-6639

Author Contributions

The manuscript was written through contributions of all authors, who all have given approval to the final version of the manuscript.

Notes

The authors declare no competing financial interest.

■ ACKNOWLEDGMENTS

The authors gratefully acknowledge the Robert A. Welch Foundation (F-1822), the ACS Petroleum Research Fund (PRF 53542-DN13), and a Cottrell Scholar Award to M.J.R. (RCSA 23640).

■ REFERENCES

(1) Braye, E. H.; Dahl, L. F.; Hübel, W.; Wampler, D. L. The preparation, properties and structure of the iron carbonyl carbide $Fe_5(CO)_{15}C$. *J. Am. Chem. Soc.* **1962**, *84*, 4633.

(2) Churchill, M. R.; Wormald, J.; Knight, J.; Mays, M. J. Synthesis and crystallographic characterization of $[Me_4N^+]_2[Fe_6(CO)_{16}C^{2-}]$, a hexanuclear carbidocarbonyl derivative of iron. *J. Am. Chem. Soc.* **1971**, *93*, 3073.

(3) Pergola, R. D.; Bandini, C.; Demartin, F.; Diana, E.; Garlaschelli, L.; Stanghellini, P. L.; Zanello, P. Characterization, redox properties and structures of the iron nitridocarbonyl clusters $[Fe_4N(CO)_{11}\{PPh(C_5H_4FeC_5H_5)_2\}]^-$, $[Fe_6N(CO)_{15}]^{3-}$ and $[Fe_6H(N)(CO)_{15}]^{2-}$. *J. Chem. Soc., Dalton Trans.* **1996**, 747.

(4) Ghosh, S.; Hogarth, G.; Kabir, S. E.; Miah, A. L.; Salassa, L.; Sultana, S.; Garino, C. Synthesis and molecular structure of $[Fe_4(CO)_{10}(\mu_4\text{-}O)(\kappa_2\text{-dppn})]$ (dppn = 1,8-bis(diphenylphosphino)-naphthalene): A missing piece in the $[M_4(CO)_{12}(\mu_4\text{-}E)]^{n-}$ (M = Fe, Ru; E = C, N, O; n = 2, 1, 0) puzzle. *Organometallics* **2009**, *28*, 7047.

(5) Taft, K. L.; Papaefthymiou, G. C.; Lippard, S. J. A mixed-valent polyiron oxo complex that models the biomineralization of the ferritin core. *Science* **1993**, *259*, 1302.

(6) Reina, R.; Rodríguez, L.; Rossell, O.; Seco, M.; Font-Bardia, M.; Solans, X. Electrophilic additions of metal fragments containing 11- and 12-group elements to the anion carbide cluster $[Fe_5MoC(CO)_{17}]^{2-}$. X-

ray crystal structures of $(NEt_4)[Fe_5MoAuC(CO)_{17}(PMe_3)]$ and $[Fe_5MoAu_2C(CO)_{17}(dppm)]$. *Organometallics* **2001**, *20*, 1575.

(7) Spatzal, T.; Aksoyoglu, M.; Zhang, L.; Andrade, S. L. A.; Schleicher, E.; Weber, S.; Rees, D. C.; Einsle, O. Evidence for interstitial carbon in nitrogenase FeMo cofactor. *Science* **2011**, *334*, 940.

(8) Lancaster, K. M.; Roemelt, M.; Ettenhuber, P.; Hu, Y.; Ribbe, M. W.; Neese, F.; Bergmann, U.; DeBeer, S. X-ray emission spectroscopy evidences a central carbon in the nitrogenase iron-molybdenum cofactor. *Science* **2011**, *334*, 974.

(9) Delgado-Jaime, M. U.; Dible, B. R.; Chiang, K. P.; Brennessel, W. W.; Bergmann, U.; Holland, P. L.; DeBeer, S. Identification of a single light atom within a multinuclear metal cluster using valence-to-core X-ray emission spectroscopy. *Inorg. Chem.* **2011**, *50*, 10709.

(10) (a) Rail, M. D.; Berben, L. A. Directing the reactivity of $[HFe_4N(CO)_{12}]^-$ toward H^+ or CO_2 reduction by understanding the electrocatalytic mechanism. *J. Am. Chem. Soc.* **2011**, *133*, 18577. (b) Taheri, A.; Thompson, E. J.; Fettinger, J. C.; Berben, L. A. An iron electrocatalyst for selective reduction of CO_2 to formate in water: Including thermochemical insights. *ACS Catal.* **2015**, *5*, 7140. (c) Taheri, A.; Berben, L. A. Tailoring electrocatalysts for selective CO_2 or H^+ reduction: Iron carbonyl clusters as a case study. *Inorg. Chem.* **2016**, *55*, 378.

(11) Tachikawa, M.; Sievert, A. C.; Muetterties, E. L.; Thompson, M. R.; Day, C. S.; Day, V. W. Metal clusters. 24. Synthesis and structure of heteronuclear metal carbide clusters. *J. Am. Chem. Soc.* **1980**, *102*, 1725.

(12) Kuppuswamy, S.; Wofford, J. D.; Joseph, C.; Xie, Z.-L.; Ali, A. K.; Lynch, V. M.; Lindahl, P. A.; Rose, M. J. Structures, interconversions, and spectroscopy of iron carbonyl clusters with an interstitial carbide: Localized metal center reduction by overall cluster oxidation. *Inorg. Chem.* **2017**, *56*, 5998.

(13) Tachikawa, M.; Geerts, R. L.; Muetterties, E. L. Metal carbide clusters synthesis systematics for heteronuclear species. *J. Organomet. Chem.* **1981**, *213*, 11.

(14) Filippou, A. C.; Rosenauer, T. A reaction pathway of $[Fe(CO)_5]$ with alkynes via ferrabicyclobutenones. *Angew. Chem., Int. Ed.* **2002**, *41*, 2393.

(15) (a) Sioda, R. E.; Cowan, D. O.; Koski, W. S. Study of the radical anion formation of some diphenylacetylenes in dimethylformamide. *J. Am. Chem. Soc.* **1967**, *89*, 230. (b) Wawzonek, S.; Wearring, D. Polarographic studies in acetonitrile and dimethylformamide. IV. Stability of anion-free radicals. *J. Am. Chem. Soc.* **1959**, *81*, 2067. (c) Cortese, N. A.; Heck, R. F. Palladium-catalyzed reductions of α,β-unsaturated carbonyl compounds, conjugated dienes, and acetylenes with trialkylammonium formates. *J. Org. Chem.* **1978**, *43*, 3985.

(16) Itoh, T.; Nagano, T.; Hirobe, M. The $[Fe_4S_4(SR)_4]^{2-}$ catalytic reduction of diphenylacetylene to *cis*-stilbene in the presence of $NaBH_4$. *Tetrahedron Lett.* **1980**, *21*, 1343.

(17) Bortoluzzi, M.; Ciabatti, I.; Cesari, C.; Femoni, C.; Iapalucci, M. C.; Zacchini, S. Synthesis of the highly reduced $[Fe_6C(CO)_{15}]^{4-}$ carbonyl carbide cluster and its reactions with H^+ and $[Au(PPh_3)]^+$. *Eur. J. Inorg. Chem.* **2017**, 3135.